PERGAMON

International Journal of Heat and Mass Transfer 43 (2000) 4447–4456

International Journal of HEAT and MASS TRANSFER

www.elsevier.com/locate/ijhmt

An exact solution for surface temperature in down grinding

Adrienne S. Lavine

University of California, Los Angeles, CA 90095-1597, USA

Received 19 July 1999; received in revised form 7 January 2000

Abstract

A model has previously been developed for heat transfer in down grinding. A numerical solution algorithm was used to solve the system of equations. In this paper, an exact solution is found for this set of equations. The effect of the location of heat generation (i.e., at wear flats or shear planes) is explored for three typical grinding conditions: conventional grinding with aluminum oxide abrasives, creep feed grinding with aluminum oxide abrasives, and conventional grinding with cubic boron nitride (CBN) abrasives. It is found that during grinding with CBN, there is a strong effect of the assumed location of heat generation.

1. Introduction

The heat generated during grinding can lead to elevated temperatures, causing thermal damage to the workpiece material. For this reason, it is important to be able to predict the temperatures which will develop during grinding, so that the process parameters can be adjusted to yield acceptable workpiece temperatures. This paper addresses heat transfer during down grinding. Fig. 1 illustrates that in down grinding, the workpiece, wheel, and fluid move in the same direction through the grinding zone of length ℓ. In our previous paper [1], a model was presented for heat transfer in down grinding. This model used Duhamel's theorem to solve the conjugate problem of heat transfer in the workpiece, grains (of the wheel), and fluid, in order to predict the workpiece surface temperature in the grinding zone. A numerical solution algorithm was used. A more efficient numerical algorithm was developed by Zhang and Faghri [2], and Ju et al. [3] solved a somewhat different thermal model of grinding, also numerically. After developing the numerical solution in [1], we realized that there is an exact, closed form solution to this problem. In this paper, we will present the closed form solution for the workpiece background temperature, valid under either of two conditions: (a) the grinding fluid remains liquid everywhere (i.e. no film boiling), or (b) film boiling occurs throughout the entire grinding zone. When film boiling occurs over a portion of the grinding zone, and is liquid over the remaining portion, we can no longer obtain a closed form solution. This will be briefly discussed.

In this paper, we also extend the model to explore the effect of the location of heat generation. Heat is generated due to friction at the "wear flats" where the grains rub over the workpiece, and due to plastic deformation at the "shear planes" where a chip is being removed (see Fig. 2). It is not well understood how the total grinding power is distributed between these locations. We define a parameter, F_{sp}, the fraction of the total grinding power which is dissipated due to plastic

E-mail address: lavine@seas.ucla.edu (A.S. Lavine).

0017-9310/00/$ - see front matter
PII: S0017-9310(00)00024-7

Nomenclature

A_{sp}	total area of shear planes divided by grinding zone area
A_{wf}	total area of wear flats divided by grinding zone area
c	specific heat
F_{sp}	fraction of total grinding power dissipated at shear planes
k	thermal conductivity
ℓ	grinding zone length
ℓ_{sp}	shear plane length
ℓ_{wf}	wear flat diameter
q	heat flux
t_c	chip thickness
T	temperature
v_s	wheel surface speed
v_w	workpiece speed
x	coordinate in direction of motion

Greek symbols

ε	fraction of energy going into some domain
ψ	influence function
ρ	density

Subscripts

av	average value over grinding zone
c	chip
f	fluid
g	grain
i	inlet, at $x = 0$
in	into workpiece
max	maximum value in grinding zone
sp	shear plane
tot	total
w	workpiece
wb	workpiece background
wc	workpiece under chip
wf	wear flat
wg	workpiece under grain

deformation at the shear planes. We then consider the dependence of the workpiece temperature on F_{sp}, for three typical grinding conditions.

2. Theoretical analysis

In [1], we used the following form of Duhamel's theorem (written here assuming only one discontinuity in the heat flux at $x = 0$):

$$T(x) - T_i = \int_0^x \frac{\partial q(\xi)}{\partial \xi} \frac{1}{h(x-\xi)}\, d\xi + \frac{q(0)}{h(x)} \quad (1)$$

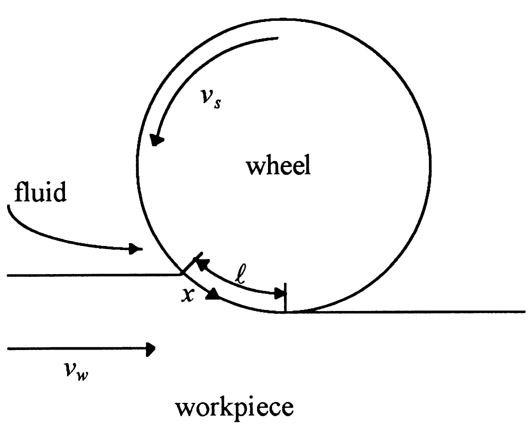

Fig. 1. Schematic drawing of down grinding.

where x is the coordinate measured along the surface of the domain, $T(x)$ is the surface temperature, T_i is the inlet temperature at $x = 0$, $q(x)$ is the heat flux into the domain at its surface, and $h(x)$ is the "heat transfer coefficient" (i.e., the ratio of heat flux, q, to surface temperature rise $T(x) - T_i$) for the case of uniform surface heat flux. In our more recent work, we have found it advantageous to work with the alternative form of Duhamel's theorem [4]:

$$T(x) - T_i = \int_0^x q(\xi) \frac{\partial \psi}{\partial x}(x-\xi)\, d\xi \quad (2)$$

where $\psi(x)$ is the influence function, equal to the reciprocal of $h(x)$ from above. We, therefore, briefly give the governing equations using this alternative form, and show how they can be combined to yield a single

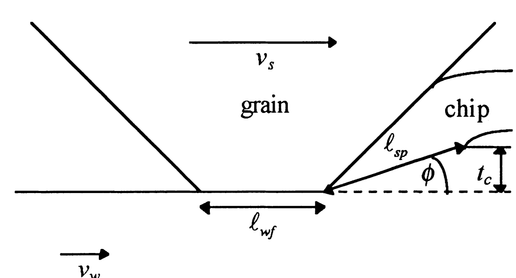

Fig. 2. Schematic drawing of grain and chip geometry.

integral equation for the workpiece background heat flux, which is in a different form from the corresponding equation in [1].

The model involves two subproblems: the wear flat problem and the workpiece background problem. The wear flat problem describes heat transfer at the interface between a grain and the workpiece (see Fig. 2). This problem consists of four equations in four unknowns, Eqs. (3)–(6), below. The first two equations express the temperatures at the wear flat for the grain and the workpiece, T_g and T_{wg}, respectively. The third equation states that these temperatures must be equal, since the grain and workpiece are in contact at the wear flat. The fourth equation indicates that the heat fluxes into the grain and workpiece, q_g and q_{wg}, add up to the total heat flux at the wear flats, q_{wf}. (Note that in our previous work [1], we called this the total grinding heat flux, q_{grind}. However, in the present work, we will later be allowing some heat generation at the shear planes, so that heat generated at the wear flats is only a portion of the total grinding power. This is the reason for the change in notation.)

$$T_g(x) - T_i = \int_0^x q_g(\xi)\frac{\partial \psi_g}{\partial x}(x-\xi)\,d\xi \tag{3}$$

$$T_{wg}(x) - T_{wb}(x) = q_{wg}(x)\psi_{wg} \tag{4}$$

$$T_g(x) = T_{wg}(x) \tag{5}$$

$$q_g(x) + q_{wg}(x) = q_{wf}(x) \tag{6}$$

Eq. (4) has a different form from the general equation (2) because ψ_{wg} is constant.

Note that the workpiece temperature rise underneath the grain (Eq. (4)) is relative to the "workpiece background temperature" (T_{wb}), that is, the temperature of the workpiece at a point which is not directly underneath a wear flat. Therefore, we need another set of equations for the workpiece background problem, Eqs. (7)–(10), below. The first two equations express the temperatures along the surface for the fluid and workpiece, T_f and T_{wb}, respectively. The third equation states that these temperatures must be equal, since the fluid is in contact with the workpiece surface (except at the wear flats). The fourth equation couples the subproblems together by stating that the heat flux which enters the workpiece under the wear flats must either remain in the workpiece (q_{wb}) or convect into the fluid (q_f).

$$T_f(x) - T_i = \int_0^x q_f(\xi)\frac{\partial \psi_f}{\partial x}(x-\xi)\,d\xi \tag{7}$$

$$T_{wb}(x) - T_i = \int_0^x q_{wb}(\xi)\frac{\partial \psi_{wb}}{\partial x}(x-\xi)\,d\xi \tag{8}$$

$$T_f(x) = T_{wb}(x) \tag{9}$$

$$A_{wf}q_{wg}(x) = q_{wb}(x) + (1 - A_{wf})q_f(x) \tag{10}$$

In Eq. (10), A_{wf} is the total area of all the wear flats divided by the grinding zone area. Considering $q_{wf}(x)$ as known, the unknowns appearing in the above equations are: q_{wg}, q_{wb}, q_g, q_f, T_{wg}, T_{wb}, T_g, and T_f. We have eight equations in eight unknowns.

The influence functions obtained from [1] are as follows:

$$\psi_{wb}(x) = 2\sqrt{x/\left(\pi(k\rho c)_w v_w\right)} \tag{11}$$

$$\psi_f(x) = 2\sqrt{x/\left(\pi(k\rho c)_f v_s\right)} \tag{12}$$

$$\psi_{wg} = \frac{4}{3}\sqrt{\ell_{wf}/\left(\pi(k\rho c)_w v_s\right)} \tag{13}$$

$$\psi_g(x) = 2g(x)\sqrt{x/\left(\pi(k\rho c)_g v_s\right)} \tag{14}$$

where

$$g(x) = \frac{\sqrt{\pi}}{2}\frac{1 - e^{G^2x}\operatorname{erfc} Gx^{1/2}}{Gx^{1/2}}, \qquad G = 2\sqrt{k_g/\left(\rho_g c_g \ell_{wf}^2 v_s\right)} \tag{15}$$

In these equations, k, ρ, and c are the thermal conductivity, density, and specific heat, respectively. The subscripts w, f, and g stand for workpiece, fluid, and grain materials. The symbols v_w and v_s are the workpiece and wheel surface speeds, respectively, and ℓ_{wf} is the diameter of an individual wear flat (see Fig. 2). Substituting Eqs. (7) and (8) into Eq. (9) yields an integral equation relating q_{wb} and q_f. Noting that ψ_{wb} and ψ_f have the same x-dependence, this equation can be reduced to $q_f = C_f q_{wb}$, where

$$C_f = \frac{\psi_{wb}}{\psi_f} = \sqrt{\frac{(k\rho c)_f v_s}{(k\rho c)_w v_w}} \tag{16}$$

Substituting this result into Eq. (10) yields $q_{wg} = Bq_{wb}$, where

$$B = \frac{1 + (1 - A_{wf})C_f}{A_{wf}} \tag{17}$$

Then, Eq. (6) results in $q_g = q_{wf} - Bq_{wb}$. Next, substituting Eqs. (3), (4) and (8) into Eq. (5), along with these expressions for q_{wg} and q_g, yields the final integral equation for q_{wb}. This can be compared with Eq. 20 of [1]. They are in different forms, but can be shown to be equivalent:

$$\int_0^x q_{wb}(\xi)\left[B\frac{\partial\psi_g}{\partial x}(x-\xi)+\frac{\partial\psi_{wb}}{\partial x}(x-\xi)\right]d\xi + B\psi_{wg}q_{wb}(x) = \int_0^x q_{wf}(\xi)\frac{\partial\psi_g}{\partial x}(x-\xi)\,d\xi \tag{18}$$

To solve for q_{wb}, we take the Laplace transform of this equation. Using overbars to denote the transform, we have:

$$\overline{q_{wb}} = \frac{\overline{q_{wf}}}{B+\left(\overline{\frac{\partial\psi_{wb}}{\partial x}}+B\overline{\psi_{wg}}\right)/\overline{\frac{\partial\psi_g}{\partial x}}} \tag{19}$$

Using Eqs. (11)–(14) for the influence functions, and taking the transforms, Eq. (19) becomes:

$$\overline{q_{wb}} = D\frac{\overline{q_{wf}}}{s^{-1/2}(s+Es^{1/2}+F)} \tag{20}$$

where

$$D = \frac{1}{B\psi_{wg}\sqrt{(k\rho c)_g v_s}} = \frac{1}{B}\frac{3}{4}\sqrt{\frac{\pi}{\ell_{wf}}} \tag{21}$$

$$E = G+\frac{1}{\psi_{wg}\sqrt{(k\rho c)_g v_s}}+\frac{1}{B\psi_{wg}\sqrt{(k\rho c)_w v_w}} = G+D(B+C_g) \tag{22}$$

$$F = \frac{G}{B\psi_{wg}\sqrt{(k\rho c)_w v_w}} = DGC_g \tag{23}$$

$$C_g = \sqrt{\frac{(k\rho c)_g v_s}{(k\rho c)_w v_w}} \tag{24}$$

For any arbitrary $q_{wf}(x)$, it may or may not be possible to invert Eq. (20) in closed form. For the particular case of linear $q_{wf}(x)$, which has been considered in previous works [1–3], i.e., $q_{wf}(x) = 2q_{wf,\,av}(1-x/\ell)$, where $q_{wf,\,av}$ is the average value of $q_{wf}(x)$ and ℓ is the length of the grinding zone, we have:

$$\overline{q_{wb}} = 2q_{wf,\,av}D\left[\frac{1}{s^{1/2}(s+Es^{1/2}+F)} - \frac{1/\ell}{s^{3/2}(s+Es^{1/2}+F)}\right] \tag{25}$$

Inverting this gives the result for the workpiece background heat flux:

$$q_{wb}(x) = \frac{2q_{wf,\,av}D}{F}\left[\frac{1}{\ell}\left(\frac{E}{F}-\frac{2}{\sqrt{\pi}}x^{1/2} - \frac{d}{a}e^{a^2x}\,\mathrm{erfc}\,ax^{1/2} - \frac{c}{b}e^{b^2x}\,\mathrm{erfc}\,bx^{1/2}\right) - \frac{F}{\sqrt{E^2-4F}}\left(e^{a^2x}\,\mathrm{erfc}\,ax^{1/2} - e^{b^2x}\,\mathrm{erfc}\,bx^{1/2}\right)\right] \tag{26}$$

where

$$a, b = \frac{E\pm\sqrt{E^2-4F}}{2} \tag{27}$$

$$c, d = \frac{\sqrt{E^2-4F}\pm E}{2\sqrt{E^2-4F}} \tag{28}$$

Based on the definitions of E and F, it can be shown that $\sqrt{E^2-4F}$ is always positive.

Finally, the workpiece background temperature can be determined from Eq. (8). The result is:

$$T_{wb}(x)-T_i = \frac{q_{wf,\,av}\ell_{wf}}{k_g}\left\{\frac{1}{\ell}\left[\frac{E}{F}\frac{2}{\sqrt{\pi}}x^{1/2} - x - \frac{d}{a^2}\left(1-e^{a^2x}\,\mathrm{erfc}\,ax^{1/2}\right) - \frac{c}{b^2}\left(1-e^{b^2x}\,\mathrm{erfc}\,bx^{1/2}\right)\right] - \frac{F}{\sqrt{E^2-4F}}\left[\frac{1}{a}\left(1-e^{a^2x}\,\mathrm{erfc}\,ax^{1/2}\right) - \frac{1}{b}\left(1-e^{b^2x}\,\mathrm{erfc}\,bx^{1/2}\right)\right]\right\} \tag{29}$$

This has been evaluated for a variety of cases and has been seen to agree with the numerical solutions presented in [1,2].

3. Heat generation at shear planes

The above solution assumes that all the grinding power is dissipated at wear flats (due to friction). In reality, some of the power is dissipated at shear planes due to plastic deformation. In this section, we develop the exact solution accounting for heat generation at shear planes, coupled with the heat transfer at wear flats in the previous section. Eq. (10) is modified to describe the fact that heat enters the workpiece under the wear flats (q_{wg}) and the shear planes (q_{wc}).

$$A_{wf}q_{wg}(x) + A_{sp}q_{wc}(x) = q_{wb}(x) + \left(1 - A_{wf} - A_{sp}\right)q_f(x) \tag{30}$$

where A_{sp} is the total area of all the shear planes divided by the grinding zone area. Next, we must develop the heat transfer problem at the shear planes [5]. The shear plane problem describes heat transfer at the interface between a chip and the workpiece (see Fig. 2). This problem consists of four equations in four unknowns, Eqs. (31)–(34), below. The first two equations express the temperatures at the shear plane for the chip and the workpiece, T_c and T_{wc}, respectively. The third equation states that these temperatures must be equal, since the chip and workpiece are in contact at the shear plane. The fourth equation indicates that the heat fluxes into the chip and workpiece, q_c and q_{wc}, add up to the total heat flux at the shear planes, q_{sp}:

$$T_c(x) - T_{wb}(x) = q_c(x)\psi_c \tag{31}$$

$$T_{wc}(x) - T_{wb}(x) = q_{wc}(x)\psi_{wc} \tag{32}$$

$$T_c(x) = T_{wc}(x) \tag{33}$$

$$q_c(x) + q_{wc}(x) = q_{sp}(x) \tag{34}$$

where the influence functions are as follows [5]:

$$\psi_c = \ell_{sp}/(\rho c)_w t_c v_s \tag{35}$$

$$\psi_{wc} = \frac{4}{3}\sqrt{\ell_{sp}/\left(\pi(k\rho c)_w v_s\right)} \tag{36}$$

In these equations, ℓ_{sp} is the length of the shear plane and t_c is the chip thickness (see Fig. 2).

Eqs. (31)–(34) can be easily solved to yield:

$$q_{wc} = \frac{\psi_c}{\psi_c + \psi_{wc}} q_{sp} \tag{37}$$

We will assume that both the wear flat and shear plane heat fluxes are linearly distributed through the grinding zone as previously. That is, $q_{wf}(x) = 2q_{wf,\,av}(1 - x/\ell)$ and $q_{sp}(x) = 2q_{sp,\,av}(1 - x/\ell)$. Furthermore, we define the total grinding heat flux, q_{tot}, to be the total grinding power divided by the grinding zone area, and let F_{sp} be the fraction of the total grinding power which is generated at the shear planes due to plastic deformation. Then, noting that all the defined heat fluxes are based on different areas, we can write that $q_{wf,\,av} = (1 - F_{sp})q_{tot}/A_{wf}$ and $q_{sp,\,av} = F_{sp}q_{tot}/A_{sp}$. Repeating the entire solution procedure outlined earlier, we can find the new expression for the workpiece background temperature, including the effect of heat generation at the shear planes. This is given below in terms of the total grinding heat flux, q_{tot}.

$$\begin{aligned} T_{wb}(x) - T_i = \frac{q_{tot}\ell_{wf}}{k_g A_{wf}} \Bigg\{ & J\Bigg\{\frac{1}{\ell}\Bigg[\frac{E}{F}\frac{2}{\sqrt{\pi}}x^{1/2} - x \\ & - \frac{d}{a^2}\left(1 - e^{a^2x}\,\mathrm{erfc}\,ax^{1/2}\right) \\ & - \frac{c}{b^2}\left(1 - e^{b^2x}\,\mathrm{erfc}\,bx^{1/2}\right)\Bigg] \\ & - \frac{F}{\sqrt{E^2 - 4F}}\Bigg[\frac{1}{a}\left(1 - e^{a^2x}\,\mathrm{erfc}\,ax^{1/2}\right) \\ & - \frac{1}{b}\left(1 - e^{b^2x}\,\mathrm{erfc}\,bx^{1/2}\right)\Bigg]\Bigg\} \\ & - K\Bigg\{\frac{1}{\ell}\Bigg[\frac{1}{F}\frac{2}{\sqrt{\pi}}x^{1/2} \\ & + \frac{c}{a^3}\left(1 - e^{a^2x}\,\mathrm{erfc}\,ax^{1/2}\right) \\ & + \frac{d}{b^3}\left(1 - e^{b^2x}\,\mathrm{erfc}\,bx^{1/2}\right)\Bigg] \\ & + \Bigg[\frac{c}{a}e^{a^2x}\,\mathrm{erfc}\,ax^{1/2} \\ & + \frac{d}{b}e^{b^2x}\,\mathrm{erfc}\,bx^{1/2}\Bigg]\Bigg\}\Bigg\} \end{aligned} \tag{38}$$

where

$$J = 1 - F_{sp} + F_{sp}H\left(1 + \frac{8}{3}\sqrt{\frac{(k\rho c)_g}{(k\rho c)_w}\frac{k_g/\rho_g c_g}{\pi\ell_{wf}v_s}}\right) \tag{39}$$

$$K = \frac{F_{sp}HC_gG}{B}\sqrt{\frac{(k\rho c)_g}{(k\rho c)_w}} \tag{40}$$

and

$$H = \frac{\psi_c}{\psi_c + \psi_{wc}} \tag{41}$$

In Eq. (38), all parameters have their definitions as given earlier, except that B is modified as follows:

$$B = \frac{1 + \left(1 - A_{wf} - A_{sp}\right)C_f}{A_{wf}} \tag{42}$$

If $F_{sp} = 0$ and $A_{sp} = 0$, then noting that under these conditions $q_{tot} = q_{wf,\,av} A_{wf}$, we recover the earlier Eq. (29).

It should be noted that the analysis presented in this section assumes that there is no heat transfer between the grain and the chip through their region of contact. The implications of this assumption will be discussed in Section 6.

4. Film boiling of grinding fluid

It has been established that grinding fluid can undergo film boiling when its temperature exceeds a critical value (referred to hereafter as the film boiling temperature). For a water based grinding fluid, the film boiling temperature is around 130°C [6]. When film boiling occurs, the heat transfer to the fluid becomes negligible. If film boiling occurs over the entire grinding zone, then the solution above is valid with C_f set to zero to eliminate heat transfer to the fluid. However, film boiling may occur over only a portion of the grinding zone. In this case, the above solution is valid in the region before film boiling occurs (i.e., before the first location at which the temperature equals the film boiling temperature), but is invalid thereafter. We have been unable to find an exact solution for the situation in which film boiling occurs over only a portion of the grinding zone. The true solution is bounded by the solutions assuming no film boiling and complete film boiling, although these bounds can be quite far apart. Of course, the solution can also be determined numerically.

5. Upgrinding

A brief word is in order regarding the difference between down grinding and upgrinding. In upgrinding, the wheel (and fluid) move in the opposite direction from the workpiece as they move through the grinding zone. This alters the nature of the mathematical problem. Without being rigorous, we can say that the down grinding problem is parabolic, since the conditions at some x depend only on the inlet conditions at $x = 0$. In contrast, the upgrinding problem is elliptic, since the conditions at some x depend on the inlet conditions at *both* ends of the grinding zone, $x = 0, \ell$. Because of this, we have not been able to find an exact solution to the upgrinding problem. However, it has been solved numerically in [7], using a much more efficient algorithm than we had used previously for down grinding in [1]. Ju et al. [3] have also solved the upgrinding problem using somewhat different model assumptions.

6. Discussion

An example of the distribution of workpiece background temperature (equal to the fluid temperature) through the grinding zone is shown in Fig. 3. The conditions are those described in Case I below, with $F_{sp} = 0.35$. It can be seen that the temperature initially increases as the workpiece and fluid are heated as they move through the grinding zone, but eventually the temperature decreases because of the decreasing heat flux. The temperature exceeds the film boiling temperature for a water based grinding fluid, but is not high enough to cause metallurgical changes (e.g., reaustenitization) for steels.

As noted earlier, this same model of grinding has been solved numerically for the case of $F_{sp} = 0$ [1,2]. Therefore, the only new results we will present here are to show the effect of F_{sp}. This effect was explored in an earlier paper [5], but using an approximate grinding model.

The distribution of the total grinding power between frictional heating at wear flats and plastic deformation at shear planes is not well known or understood, and is difficult to determine experimentally. Malkin and Anderson [8] have measured the grinding power as a function of wear flat area. Extrapolating this curve to zero wear flat area should give the rate of heat generation at shear planes. Then, for realistic values of wear flat area, the percentage of the total grinding power

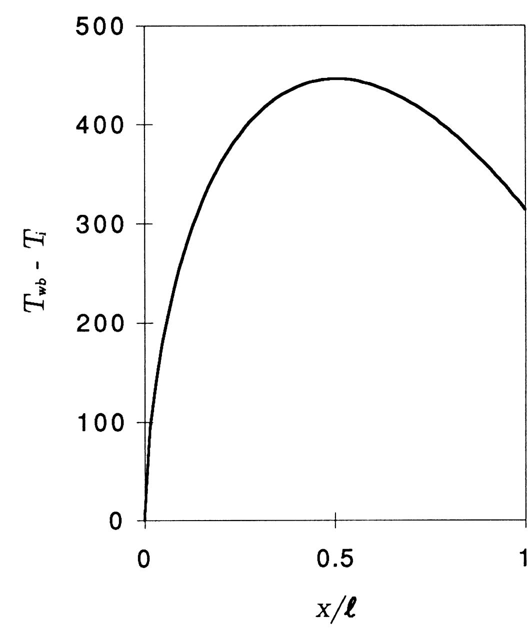

Fig. 3. Sample workpiece background temperature distribution.

which is dissipated at shear planes can be determined. For conventional grinding conditions, using conventional abrasives, Malkin and Anderson's data suggest a typical value of about 35% for the shear plane heat generation. This percentage would change as a function of all the parameters describing the grinding conditions, such as wheel dressing conditions, depth of cut, type of abrasive, etc. For example, F_{sp} would probably be higher for grinding with cubic boron nitride (CBN) abrasives, since they tend to be sharper, and therefore, generate less heat at wear flats due to friction.

We will explore the effect of F_{sp} by considering three types of grinding.

- Case I: conventional grinding conditions with aluminum oxide abrasive.
- Case II: creep feed grinding conditions (low workpiece speed, large depth of cut) with aluminum oxide abrasive.
- Case III: conventional grinding conditions with CBN abrasive.

The grinding conditions are shown in Table 1. The conventional grinding conditions with both aluminum oxide and CBN abrasives are taken from the experimental conditions of Kohli et al. [9]. These experimental conditions were for upgrinding, but we use them here as an example for down grinding. The creep feed grinding conditions are identical to the conventional grinding conditions with aluminum oxide abrasive, except that the workpiece speed is lowered to $v_w = 1$ mm/s and the depth of cut is raised to give the same material removal rate (which increases the grinding zone length, ℓ). The grinding power is assumed to be the same, since to first order it is dependent on material removal rate. (These same conditions were investigated by Ju et al. [3] using a different grinding model.) Demetriou and Lavine [7] explain how the values of the parameters describing the small scale geometry of grains and chips (i.e., A_{wf}, ℓ_{wf}, A_{sp}, ℓ_{sp}, t_c) are determined from the given wheel specification and grinding conditions.

When the temperature was calculated for Case I assuming that the grinding fluid remained liquid, the temperature was seen to exceed the film boiling temperature of 130°C throughout the large majority of the grinding zone. This is typical of conventional grinding with aluminum oxide abrasives. Therefore, it was subsequently assumed that the grinding fluid would boil everywhere, the heat transfer to the fluid was set to zero, and the temperature was recalculated. On the other hand, temperatures for Cases II and III typically remained below the film boiling temperature (with some exceptions), so those cases were run assuming that the grinding fluid remained liquid throughout the grinding zone.

For each of these three cases, we calculate the workpiece background temperature for varying F_{sp}. The results for the maximum workpiece background temperature rise ($T_{wb,\,max} - T_i$) are shown in Fig. 4. The results show the sensitivity of the predicted temperature to F_{sp}, i.e., the error incurred by not knowing F_{sp}

Table 1
Input data for three grinding cases

	Case I	Case II	Case III
k_w (W/m K)	60.5	60.5	60.5
ρ_w (kg/m^3)	7854	7854	7854
c_w (J/kg K)	434	434	434
k_f (W/m K)		0.68	0.68
ρ_f (kg/m^3)	No fluid	1000	1000
c_f (J/kg K)		4180	4180
k_g (W/m K)	46	46	1300
ρ_g (kg/m^3)	4000	4000	3450
c_g (J/kg K)	770	770	506
v_s (m/s)	30	30	30
v_w (mm/s)	150	1.0	135
ℓ (mm)	2.5	30.6	2.5
Grinding power (W)	1670	1670	1280
q_{tot} (W/mm^2)	66.8	5.45	51.2
A_{wf}	0.009	0.009	1.8×10^{-5}
ℓ_{wf} (μm)	63	63	1.0
A_{sp}	5.7×10^{-4}	5.7×10^{-4}	5.2×10^{-4}
ℓ_{sp} (μm)	12	12	4.0
t_c (μm)	1.0	1.0	0.34

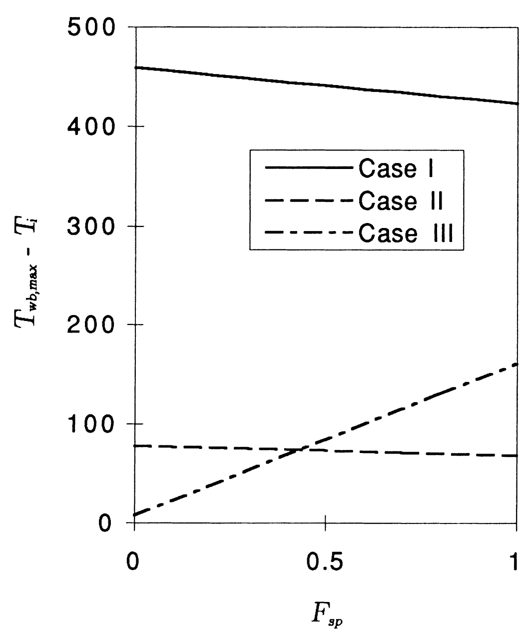

Fig. 4. Maximum temperature vs. F_{sp}.

accurately. It can be seen that for both conventional and creep feed grinding conditions with aluminum oxide abrasives (Cases I and II), there is very little dependence on F_{sp}. Temperature decreases slightly with increasing F_{sp}: the range is only 36°C for Case I and 10°C for Case II. On the other hand, for conventional grinding conditions with CBN abrasives (Case III), the temperature increases rapidly with increasing F_{sp}, with a range of 153°C. For values of F_{sp} greater than about 0.6, water based grinding fluid would undergo film boiling, and the temperature would be even higher than what is shown.

We will now discuss and explain the dependence of the workpiece background temperature on F_{sp}. The grinding heat transfer problem is clearly a coupled problem of conduction in the wheel, workpiece, and fluid. We can imagine decoupling the problems so that we isolate the workpiece background heat transfer problem (Eqs. (7)–(9), (30)) with specified heat input to the workpiece at the wear flats and shear planes (q_{wg}, q_{wc}). From this perspective, F_{sp} affects the problem because it affects q_{wg} and q_{wc}. More specifically, it affects the left-hand side of Eq. (30), which is an expression for the total heat flux entering the workpiece. As a means to understand the effect of F_{sp}, we will examine the total *rates* at which heat enters the workpiece (ignoring the dependence on the distribution of the heat flux with x) at the wear flats and shear planes.

We define ε_{wg} as the fraction of the heat generated at the wear flats which enters the workpiece under the grains, and ε_{wc} as the fraction of the heat generated at the shear planes which enters the workpiece under the chips. Then the fraction of the total grinding power which enters the workpiece, ε_{in}, is given by:

$$\varepsilon_{in} = \varepsilon_{wg}\left(1 - F_{sp}\right) + \varepsilon_{wc}F_{sp} \tag{43}$$

For future discussion, we also define ε_{wb} as the fraction of the total grinding power which remains in the workpiece and ε_f as the fraction of the total grinding power which is removed by the fluid. Then, $\varepsilon_{wb} + \varepsilon_f = \varepsilon_{in}$. All of these "fractions" are referred to as "partitions" in the figure titles which follow.

Fig. 5 shows ε_{wg}, ε_{wc}, and ε_{in} as functions of F_{sp} for Cases I and II. It can be seen that the two cases exhibit very similar behavior. In fact, ε_{wc} is the same constant value for both cases; it can be shown that $\varepsilon_{wc} = H$ (see Eqs. (37) and (41)), and H depends only on workpiece properties, shear plane geometry, and wheel speed, which are all the same for Cases I and II. The fact that ε_{wc} is constant can be explained on physical grounds because both the heat flux to the chip and the heat flux to the workpiece under the chip are proportional to the same temperature difference, $T_{wc} - T_{wb}$ (cf. Eqs. (31)–(33)). Therefore, the fraction of heat entering the workpiece under the chip is independent of this temperature difference and thus independent of F_{sp}.

In contrast, considering heat transfer at the wear flats, the heat flux to the grain depends on $T_{wg} - T_i$ and the heat flux to the workpiece under the grain is proportional to $T_{wg} - T_{wb}$ (cf. Eqs. (3)–(5)), resulting in a non-constant ε_{wg}. It can be seen that ε_{wg} is negative for F_{sp} greater than approximately 0.8. The reason is that as F_{sp} increases, the grinding power is being moved away from the wear flats and to the shear planes (by definition of F_{sp} as the fraction of heat generated at shear planes). The temperature at the shear planes (T_{wc}) therefore increases, and the temperature at the wear flats (T_{wg}) decreases. When T_{wg} decreases below T_{wb}, heat can conduct from the workpiece to the wear flat; this corresponds to negative ε_{wg}. Then all of the heat generated at the wear flats, *plus* some additional heat coming from the workpiece, can enter the cooler grains.

We can also see that ε_{in} lies between ε_{wc} and ε_{wg}, as it must, since it is a weighted average of the two. For F_{sp} near zero, ε_{wg} and ε_{wc} are fairly close to each other, so the weighted average does not change much as F_{sp} changes. Then, as ε_{wg} begins to decrease rapidly, it does not cause large variation in ε_{in}, because $1 - F_{sp}$ is becoming small. It appears from a cursory look at Eq. (43) that when $F_{sp} = 1$, ε_{in} should be equal to ε_{wc}. However, the reality is that, as F_{sp} goes to 1, ε_{wg} approaches $-\infty$, and the quantity ε_{wg} $(1 - F_{sp})$ is finite

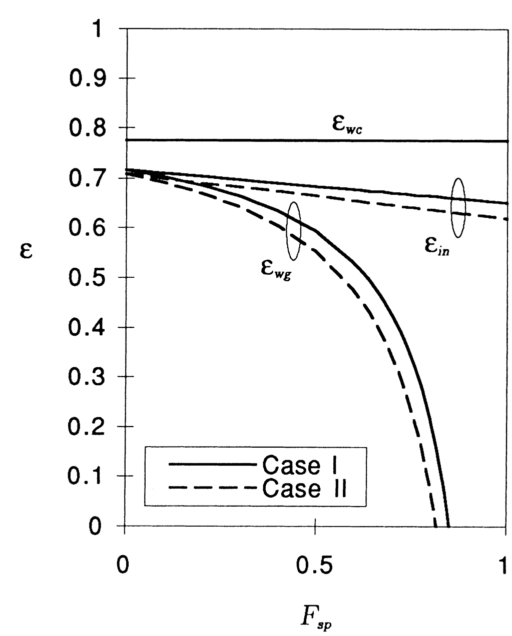

Fig. 5. Partitions for Cases I and II.

and non-zero. Physically, we can understand that when F_{sp} goes to 1 it does not mean that heat transfer to the workpiece is determined only by what is happening at the shear planes. Rather, the wear flats still play a role by providing a path for heat transfer from the workpiece to the grains, thereby reducing ε_{in}.

Fig. 6 shows the same kind of results for Case III. The situation here is very different. Because of the high thermal conductivity of CBN grains, much more of the heat generated at the wear flats goes to the grains than to the workpiece under the grains. Therefore, ε_{wg} is very small. It shows a decreasing trend as in the other cases, and again it approaches $-\infty$ as F_{sp} goes to 1, although it remains nearly constant over a broader range of F_{sp}. Since the magnitudes of ε_{wc} and ε_{wg} are very different, as F_{sp} varies, ε_{in} varies significantly, increasing with increasing F_{sp}. Although it appears that $\varepsilon_{in} = \varepsilon_{wc}$ when $F_{sp} = 1$, it is not an exact equality. Just as in Cases I and II, $\varepsilon_{wg}(1 - F_{sp})$ is non-zero (but small) when $F_{sp} = 1$.

To reiterate, when grinding with CBN abrasives, the fraction of heat going to the workpiece at the wear flats is much less than the fraction of heat going to the workpiece at the shear planes. Thus, the assumed value of F_{sp} has a dramatic effect on the total heat entering the workpiece and consequently on the workpiece background temperature.

Recall that the analysis assumed no heat transfer between the grain and the chip through their region of contact. In reality, conduction would tend to reduce the temperature difference between the grain and the chip and consequently reduce the dependence on F_{sp}. A detailed analysis has been performed of the effect of conduction between the grain and the chip. Without presenting it here, the conclusions will be briefly summarized. First, it should be noted that conduction between the grain and the chip is strongly dependent on their contact area, which is not well known. This contact area was assumed equal to the shear plane area. Accounting for grain–chip conduction was found to have a negligible effect on the workpiece background temperature for Cases I and II (which already showed little dependence on F_{sp}). For Case III (CBN grains), the effect of grain–chip conduction was significant. Recalling from Fig. 4 that the temperature range for Case III was 153°C, this temperature range would be reduced approximately to half by the effect of conduction between the grain and the chip. Despite this reduction, the effect of F_{sp} on workpiece background temperature would still be much more significant for Case III than for Cases I and II.

Next, comparing Cases I and II, recall that they were assumed to have the same grinding power, and their values for ε_{in} are very similar (Fig. 5), so heat enters the workpiece at about the same rate. It is then reasonable to ask why their workpiece background temperatures are so different (cf. Fig. 4). The reason stems from the different grinding zone lengths (see

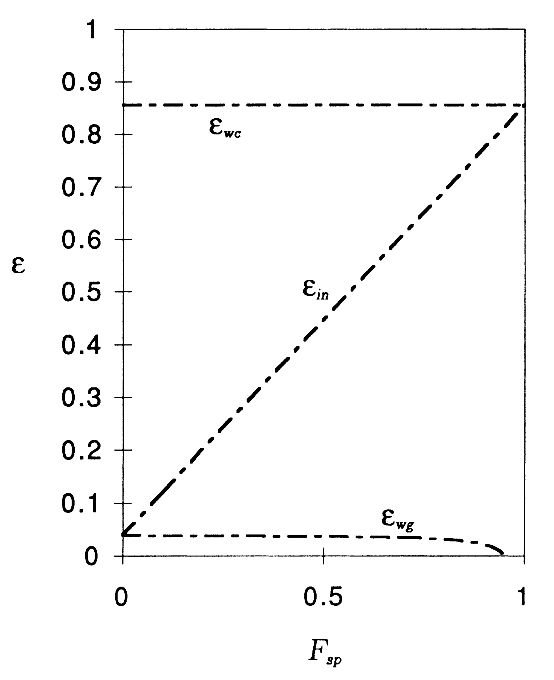

Fig. 6. Partitions for Case III.

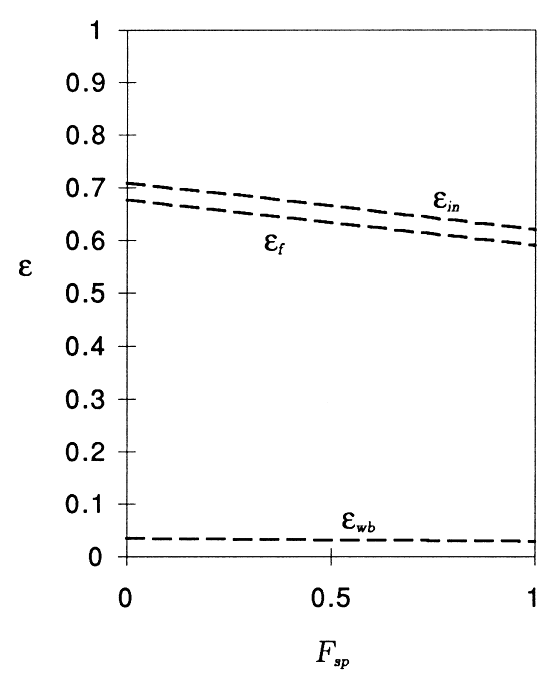

Fig. 7. Workpiece and fluid partitions for Case II.

Table 1). Since the grinding zone length is much shorter for conventional grinding (Case I) than for creep feed grinding (Case II), the *heat flux* entering the workpiece is much greater. This results in a much higher workpiece temperature in conventional grinding. If this were the only effect at work, the temperature rise would scale as $\ell^{-1/2}$ due to the changes in heat flux and ψ_{wb} (see Eqs. (8) and (11)). This results in temperature rises for conventional grinding which are higher than those in creep feed grinding by a factor of 3.5. The temperature rise in creep feed grinding is on the order of 70°C (as seen in Fig. 4), so the temperature rise in conventional grinding would be around 250°C. But since these temperatures are high enough to cause film boiling of the grinding fluid, the heat loss to the fluid becomes negligible, resulting in even higher temperatures in conventional grinding, as shown in Fig. 4. Thus, for Case I, the fraction of the grinding power which enters the workpiece is the same as the fraction which remains in the workpiece, i.e., $\varepsilon_{in} = \varepsilon_{wb}$. In contrast, for Case II, $\varepsilon_{wb} < \varepsilon_{in}$. Fig. 7 shows ε_{in}, ε_{wb}, and ε_f for Case II. Much more heat is removed by the fluid than by the workpiece itself, because the fluid travels much faster, more than compensating for its lower thermal conductivity.

Acknowledgements

The author appreciates the support of the National Science Foundation through various grants. Also, thanks to the late Prof. G.C. Pomraning for the suggestion to use Laplace transforms.

References

[1] T.-C. Jen, A.S. Lavine, A variable heat flux model of heat transfer in grinding: model development, J. Heat Transfer 117 (1995) 473–478.
[2] Y. Zhang, A. Faghri, An integral approximate solution of heat transfer in the grinding process, Int. J. Heat Mass Transfer 39 (1996) 2653–2662.
[3] Y. Ju, T.N. Farris, S. Chandrasekar, Theoretical analysis of heat partition and temperatures in grinding, J. Tribology 120 (1998) 789–794.
[4] J.V. Beck, et al., Heat Conduction Using Green's Functions, Hemisphere, Washington, DC, 1992.
[5] A.S. Lavine, Thermal aspects of grinding: the effect of heat generation at the shear planes, CIRP Annals 40 (1991) 343–345.
[6] T.-C. Jen, A.S. Lavine, A variable heat flux model of heat transfer in grinding with boiling, J. Heat Transfer 118 (1996) 463–470.
[7] M.D. Demetriou, A.S. Lavine, Thermal aspects of grinding: the case of upgrinding, J. Manuf. Sci. and Eng. 122 (2000).
[8] S. Malkin, R.B. Anderson, Thermal aspects of grinding. Part 1 — energy partition, J. Eng. Ind. 96 (1974) 1177–1183.
[9] S. Kohli, C. Guo, S. Malkin, Energy partition to the workpiece for grinding with aluminum oxide and CBN abrasive wheels, J. Eng. Ind. 117 (1995) 160–168.